

# Wall heat flux measurements behind a shock wave generated by a detonation

Virof F., Quintens H., Boust B., Sotton J., Bellenoue M.

*PPrime Institute, CNRS, ISAE-ENSMA, Université de Poitiers*

*1 avenue Clément Ader, BP 40109*

*86961 Futuroscope Chasseneuil Cedex, France*

## 1 Introduction

Aeronautic turbo-engines are currently under major investigation to improve their efficiency and reduce the emission of pollutants and greenhouse effect gas. It was already demonstrated that the optimization of the current propulsive system would not be sufficient to reach the emission reduction goals claimed by regulation organizations. Thus, innovative propulsive solutions are investigated that use Pressure Gain Combustion (PGC) and more particularly detonation to oxidize the mixture. Rotating Detonation Engine (RDE) seems to be a promising solution and is studied world-wide but to access the real performance of such engine, a thermal characterization is needed to evaluate the thermal losses generated during its operation. Paxson *et al.* have measured the mean heat losses through the wall by using a water-cooling system and by recording the coolant temperature variation between the input and the output of the system [1]. However, in this configuration, the influence of the detonation itself is not separated from the influence of the burnt gases on the thermal losses. Several studies try to implement a local wall heat flux measurement to investigate the thermal flux generated by the propagation of a detonation in a canonical configuration [2] [3] and in a RDE [4]. However, the obtained results are extremely dispersed from  $10 \text{ MW}\cdot\text{m}^{-2}$  to  $200 \text{ MW}\cdot\text{m}^{-2}$ . Using NANMAC thermocouples, Quintens *et al.* showed that the heat flux peak, associated to the detonation, could be resolved using an acquisition frequency of at least 62 MHz [5].

This work aims at studying the influence of the shock velocity on the wall heat flux generated during its propagation in a canonical experimental setup, in which the shock in air is generated by the propagation of a steady detonation [6].

## 2 Experimental setup

Experiments are conducted in a 52 mm-inner diameter stainless steel tube and about 8 m-long, closed at both ends (cf Figure 1). A 100  $\mu\text{m}$ -thick plastic film (Mylar) splits the tube in two parts: on the left, a driver section of 6 m-long is filled with stoichiometric  $\text{H}_2/\text{O}_2$  mixture and, on the right, air at ambient pressure rests in the driven section.

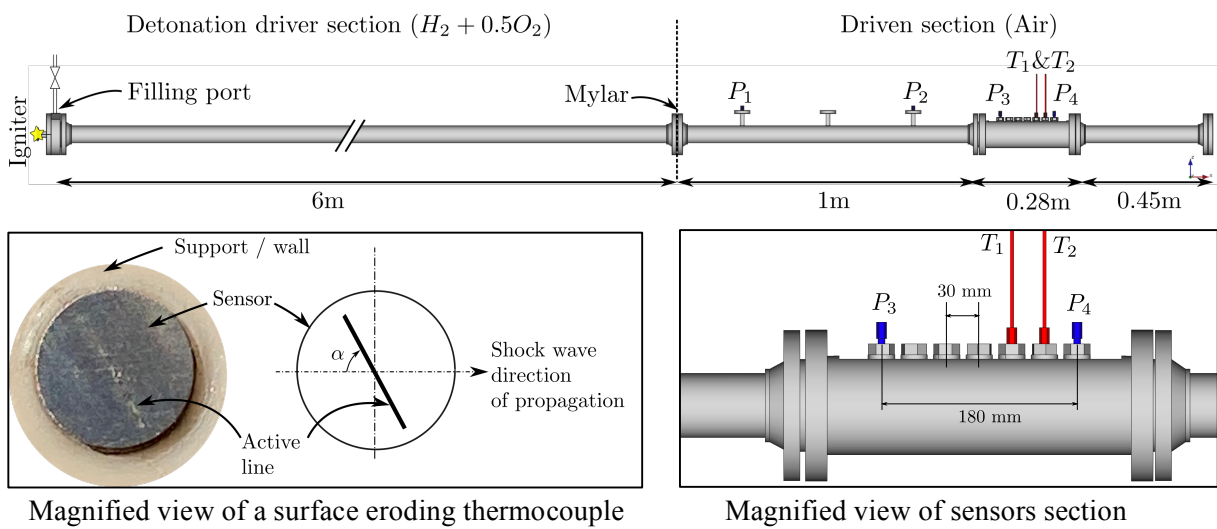


Figure 1 Sketch of the experimental setup with pressure sensors (in blue) and thermocouples (in red)

Pressure is measured by four Kistler 603B sensors along with their Kistler 5011 charge amplifiers ( $P_1$  to  $P_4$ ) while wall surface temperature is given by two type-E eroding thermocouples ( $T_1$  and  $T_2$ , NANMAC) between the last two pressure sensors (see magnified view of Figure 1). All the sensors are flush mounted. Distances between pressure sensors are  $d_{P_1-P_2} = 580$  mm,  $d_{P_2-P_3} = 280$  mm and  $d_{P_3-P_4} = 180$  mm respectively.

Signals are recorded on a Tektronix MSO56 oscilloscope at 62.5 MHz with High Resolution mode (16 bits) and a 20 MHz bandwidth.

The driver section is vacuumed below 200 Pa before it is filled by the reactive mixture at initial pressure  $P_0$  from a 50 L tank. This is controlled by a static pressure gauge (Keller PA33X). Mixtures are prepared with partial pressure method in a specific device at least two hours and the bottles are rotated before use in order to ensure a complete species diffusion.

An electric igniter is fired on the left end of the tube end to start the detonation. As the detonation propagates to the right by consuming the reactive mixture, a shock wave is generated in the inert gas when interacting with the driven section. Thanks to the high pressure increase in the detonation wave, this method is known to produce stronger shocks as in classical shock tube; nevertheless, the post shock pressure is not so much maintained due to the presence of the expansion wave just after the detonation front.

### 3 Experimental operating conditions

Initial pressure  $P_0$  is ranging from 50 kPa to 100 kPa. A self-sustained quasi-CJ detonation ( $D/D_{CJ}=0.99$ ) propagates in the driver section then interacts with the air in the driven section. Table 1 summarizes the theoretical characteristics of the detonation obtained with SDT toolbox [7] and experimental ones for shock propagation. The instantaneous shock velocity is determined from a second order polynomial law taking into account the shock time arrival on pressure sensors and Hugoniot post-shock relations are used to calculate  $P$  and  $T$  on  $P_4$ . The decrease of velocity between  $T_1$  and  $P_4$  is, at worse, below 1.4 %.

Table 1 CJ detonation and experimental shock wave parameters

$P_0$ (kPa)	$D_{CJ}$ (m/s)	$P_{CJ}$ (MPa)	Shock velocity at $P_4$ (m/s)	Post-shock $P$ at $P_4$ (kPa)	Post-shock $T$ at $P_4$ (K)	Shock Mach number at $P_4$ (-)
50	2800	0.93	737	509	533	2.14
75	2822	1.42	897	765	657	2.61
90	2832	1.71	1013	982	758	2.95
100	2838	1.91	1059	1075	801	3.08

Figure 2 shows typical pressure and temperature signals recorded during a test. The incident shock wave crosses successively the pressure sensors, which is indicated by successive pressure jumps. The pressure behind the shock wave decreases as the wave propagates in the tube meaning that its velocity is slightly decreasing; this is confirmed by an (x,t) diagram. From  $t > 1.5$  ms, the reflected shock wave produces a second pressure jump of lower intensity. Thermocouples have been plugged directly to the oscilloscope without amplifier to avoid any signal losses due to low-pass filtering. On the other hand, it induces low amplitude signals to record. That is why some noise appears around the temperature signal. A second order digital Butterworth filter on oversampled data is applied to the recorded temperature signals. The heat flux is then calculated using the method described in the next section.

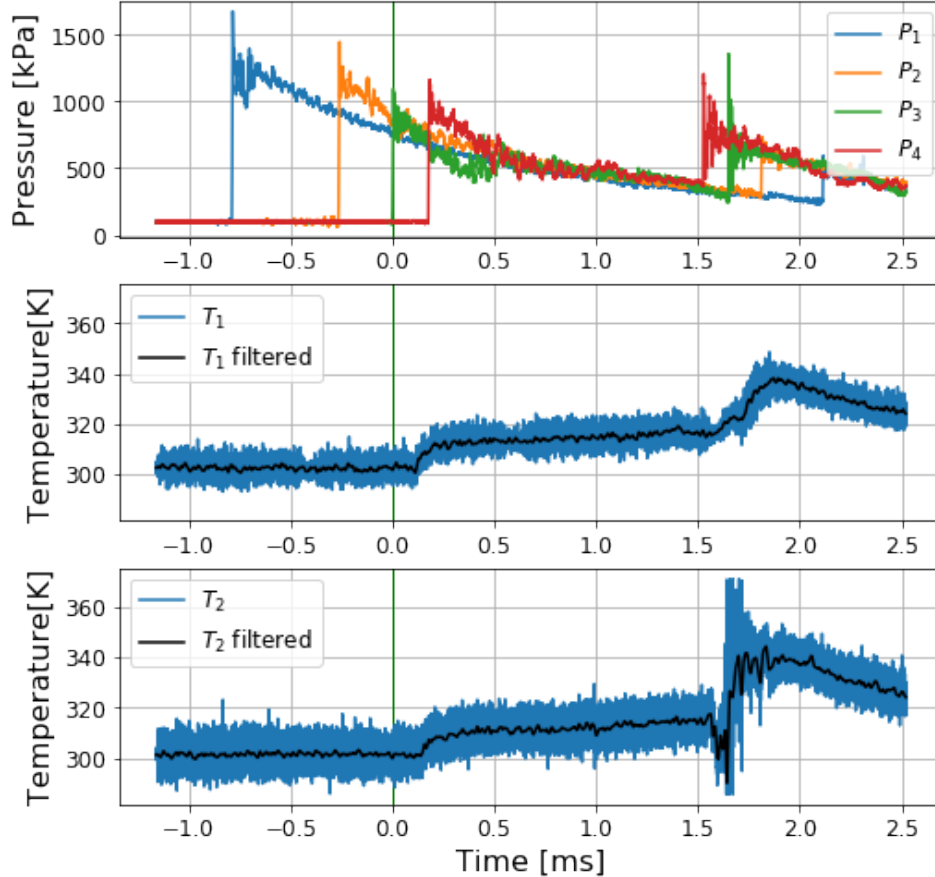


Figure 2 Pressure and temperature signals recorded for  $P_0 = 90$  kPa; temperature signal filtered using a digital second order Butterworth filter with 0.001 half-cycles / sample.

#### 4 Wall heat flux calculation

As seen on Figure 2, a transient temperature evolution is recorded by the surface thermocouples when the shock wave goes over the sensors. Short duration of the experiment allows an unsteady one-dimensional heat conduction model being used in a semi-infinite wall where temperature given by thermocouples defines the boundary condition. This technique has been already implemented in flame quenching studies by Boust *et al.* [8] and leads to evaluate the following integro-differential equation:

$$q_w(t) = q_0 + \sqrt{\frac{k\rho C_p}{\pi}} \int_{\tau=0}^t \frac{\partial T_w}{\partial \tau}(\tau) \frac{d\tau}{\sqrt{t-\tau}} \quad (1)$$

Following the numerical development presented by Bellenoue *et al.* [9], the heat flux  $Q_w$  can be calculated as a function of the measured voltage  $U$ , taking into account the Seebeck coefficient  $S$ , the thermal effusivity of the material  $\epsilon$ :

$$Q_w(t_n) = \frac{2}{\sqrt{\pi}} \frac{\epsilon \cdot S}{\Delta t} \sum_{i=0}^n U_i f_i \quad \text{with} \quad f_i = \begin{cases} \sqrt{n} - \sqrt{n-1} & i = 0 \\ \sqrt{n-i+1} - 2\sqrt{n-i} + \sqrt{n-i-1} & \text{for } i \in [1: n-1] \\ 1 & i = n \end{cases} \quad (2)$$

The values of thermal effusivity  $\epsilon$  and Seebeck coefficient  $S$  are set to  $10 \text{ kJ/K.m}^2.\text{s}^{1/2}$  and  $70 \text{ } \mu\text{V/K}$  respectively for the postprocessing.

Postprocessing a noisy signal with this algorithm returns unusable results since its behavior is like a derivative filter. Filtering is mandatory and the effect of cutoff parameter in filtering is presented in Figure 3. When the shock wave hits the sensor at time marked by the vertical blue line, a rapid increase of the temperature along with a high value of the flux (peak) is recorded. Signal is all the smoother as the  $w$  parameter is low. Grudgingly, too low values such as  $w=0.0001$  damp high frequencies needed to resolve flux peaks and, following the red curve for temperature, the temperature starts to increase before the shock arrival contrary to the black curve. Other filters have also been tested like the simple moving average and similar results can be obtained by adjusting the window width (not shown here).

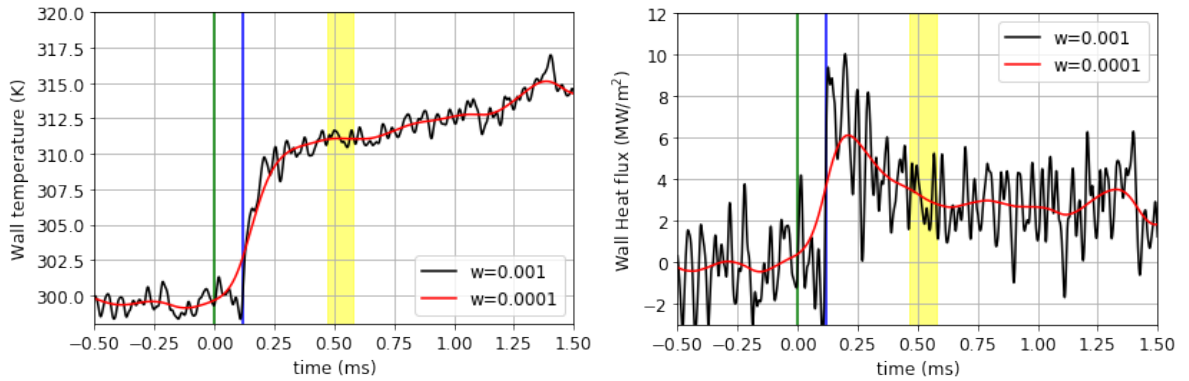


Figure 3 Wall temperature  $T_1$  (left) and calculated heat flux for two cutoff coefficient  $w$  of the second order Butterworth filter (in half-cycles / sample) (right) and for  $P_0 = 90 \text{ kPa}$ . The green vertical line corresponds to the oscilloscope reference trigger time (on  $P_3$ ) although blue one gives the shock arrival on  $T_1$ . Yellow area indicates the estimation of the contact surface passage on  $T_1$ .

## 5 Experimental results

Wall heat flux plotted on Figure 3 and obtained for  $P_0 = 90 \text{ kPa}$  jumps at  $8 \pm 2 \text{ MW/m}^2$  as the shock wave passes over the sensor then decreases until  $t \approx 0.5 \text{ ms}$  and stabilizes at  $3 \pm 1.1 \text{ MW/m}^2$ . Slope change in flux corresponds to contact surface arrival where detonation products at high temperature arrive.

Figure 4 shows the evolution of the heat flux calculated from the different temperature signals. The flux is all the more important as the strength of the incident shock increases (i.e.  $P_0$  increases). Likewise, when the reflected shock wave hits the sensors, a flux peak is obtained and its amplitude is higher than the one from the incident shock wave for pressure higher than  $90 \text{ kPa}$ .

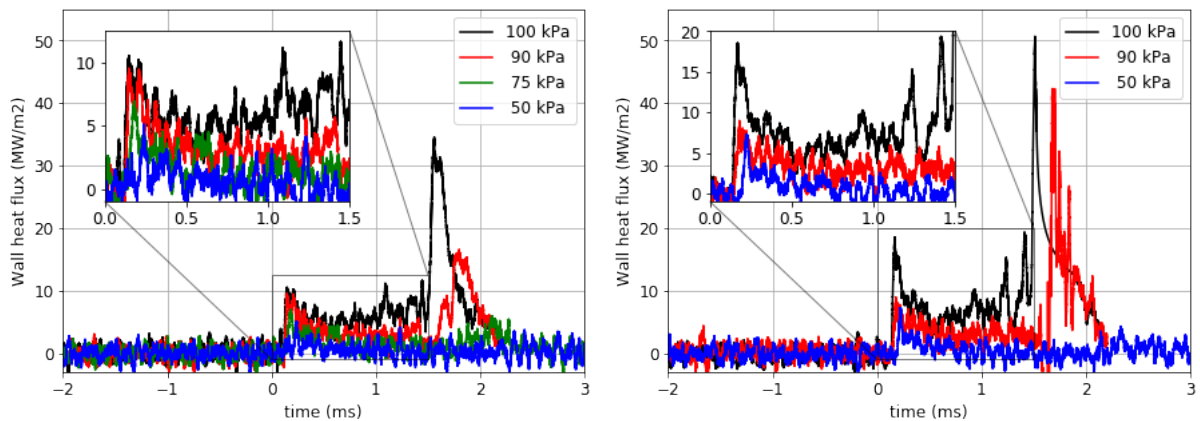


Figure 4 Wall heat flux calculation from  $T_1$  signal (left) and  $T_2$  signal (right) in function of  $P_0$

Peak values caused by the incident shock wave are graphically summarized as a function of the post shock temperature on Figure 5. At low pressure, peak values are similar for both thermocouples, besides at high pressure, it seems that the thermocouple  $T_2$  records larger heat flux peaks: this might be explained by the orientation of the sensor relative to the shock propagation (see Figure 1). Further experiments are needed and will be reported.

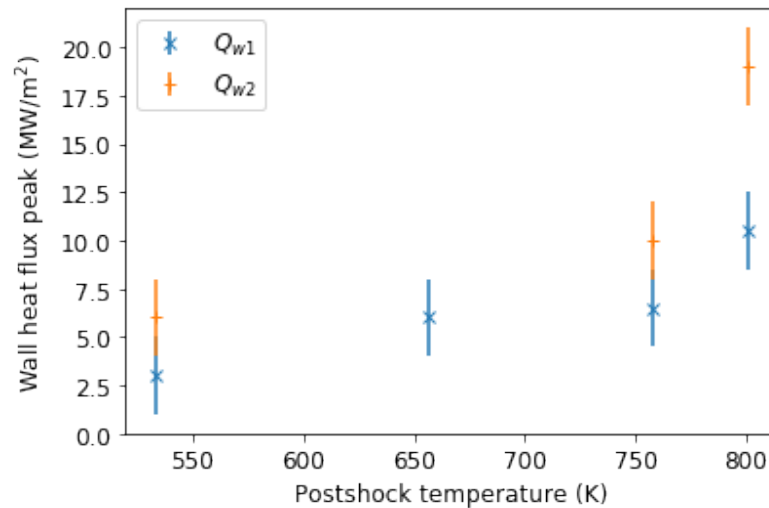


Figure 5 Wall heat flux peak values in function of the post shock temperature.

## 5 Conclusion

Experiments have been conducted in a 52-mm inner diameter shock tube with a detonation driver. The initial pressure of the stoichiometric  $H_2/O_2$  mixture in the driver section is varied to generate different shock strengths. Heat flux is recorded on the inner wall surface using eroding junction type-E thermocouples (NANMAC).

Heat flux peaks from  $3 \text{ MW}\cdot\text{m}^{-2}$  to  $19 \text{ MW}\cdot\text{m}^{-2}$  were measured on the wall when a non-reacting shock propagates between Mach 2 to Mach 3. The peak amplitude is directly linked to the post shock pressure. More tests are needed to establish a complete correlation.

The influence of the sensor orientation relative to the shock propagation will also be investigated in terms of amplitude of the wall heat flux peak.

## Acknowledgement

This work is part of the CAPA industrial chair between SAFRAN Tech, MBDA France and the ANR. The authors would like to acknowledge S. Ilango and R. D'Ayer for their participations to the test campaign during their internship. The authors are also grateful to CPER for funding a part of the experimental setup used for this study.

## References

- [1] D. Paxson, A. Naples, J. Hoke and F. Schauer, "Numerical analysis of a pulse detonation cross flow heat load experiment," in *49th AIAA Aerosp. Sci. Meet. Incl. New Horizons Forum Aerosp. Expo*, 2011.
- [2] D. Kublik, J. Kindracki and P. Wolanski, "Evaluation of wall heat loads in the region of detonation propagation of detonative propulsion combustion chambers," *Applied Thermal Engineering*, no. April, 2019.
- [3] H. Quintens, Q. Michalski, J. Moussou, C. Strozzi, J. Sotton, M. Bellenoue, B. Boust, G. Pilla and F. Rabeau, "Experimental wall heat transfer measurements for various combustion regimes: Deflagration, autoignition and detonation," in *AIAA Propulsion and Energy Forum*, Indianapolis, 2019.
- [4] F. Bykovskii and E. Vedernikov, "Heat fluxes to combustor walls during continuous spin detonation of fuel air mixtures," *Combustion Explosions and Shockwaves*, vol. 45, no. 1, pp. 70-77, 2009.
- [5] H. Quintens, Q. Michalski, F. Viro, B. Boust, Sotton and B. M. J., "Experimental investigation of the unsteady wall heat flux during self sustained detonation propagation," in *AIAA Propulsion and Energy*, Virtual, 2021.
- [6] T. Bazhenova and R. Souloukhin, "Gas ignition behind shock waves," *Proceedings of the combustion institute*, vol. 7, p. 866.
- [7] S. Browne, J. Ziegler and J. Shepherd, "Numerical Solution Methods for Shock and Detonation Jump Conditions," California Institute of Technology, 2018.
- [8] B. Boust, J. Sotton, S. Labuda and M. Bellenoue, "A thermal formulation for single-wall quenching on transient laminar flames," *Combustion and Flame*, vol. 143, no. 3, pp. 286-294, 2007.
- [9] M. Bellenoue, B. Boust and J. Sotton, "Unsteady Contribution of water vapor condensation to heat losses at flame-wall interaction," in *6th European Thermal Sciences Conference EURO THERM*, Poitiers, 2012.